Enhanced particulate Hg export at the permafrost boundary, western Siberia

Artem G. Lim, Jeroen E. Sonke, Ivan V. Krickov, Rinat M. Manasypov, Sergey V. Loiko, Oleg S. Pokrovsky

Enhanced particulate Hg export at the permafrost boundary, western Siberia

Artem G. LIM[1], Jeroen E. SONKE[2], Ivan V. KRICKOV[1], Rinat M. MANASYPOV[1],

Sergey V. LOIKO[1], Oleg S. POKROVSKY[2,3*]

[1] *BIO-GEO-CLIM Laboratory, Tomsk State University, Tomsk, 634050, Russia*
[2] *Geosciences and Environment Toulouse, CNRS, Université Paul Sabatier, 14 Avenue Edouard Belin 31400 Toulouse, France*
[3] *N. Laverov Federal Center for Integrated Arctic Research, IEPS, Russian Academy of Sciences, 163000 Arkhangelsk, Russia*

**Email: oleg.pokrovsky@get.omp.eu*

Key words: particulate, suspended, landscape, bog, lake, forest, thaw, Siberia

Submitted to *Environmental Pollution,* after 2nd revision, August 2019

Bullet points:

- Particulate Hg (PHg) concentration in western Siberia rivers decreases with watershed size
- PHg correlates with organic carbon and anti-correlates with lithogenic elements
- Hg mobilization from organic (peat) rather than mineral soil layers to the rivers
- Maximum PHg concentration and export fluxes in the sporadic permafrost zone
- Climate warming and permafrost thaw may double PHg export to the Arctic Ocean

Capsule:

Enhanced Hg mobilization from peat soil to the rivers at the permafrost boundary, due to maximal depth of the thawed layer

Abstract

Arctic permafrost soils contain large amounts of organic carbon and the pollutant mercury (Hg). Arctic warming and associated changes in hydrology, biogeochemistry and ecology risk mobilizing soil Hg to rivers and to the Arctic Ocean, yet little is known about the quantity, timing and mechanisms involved. Here we investigate seasonal particulate Hg (PHg) and organic carbon (POC) export in 32 small and medium rivers across a 1700 km latitudinal permafrost transect of the western Siberian Lowland. The PHg concentrations in suspended matter increased with decreasing watershed size. This underlines the significance of POC-rich small streams and wetlands in PHg export from watersheds. Maximum PHg concentrations and export fluxes were located in rivers at the beginning of permafrost zone (sporadic permafrost). We suggest this reflects enhanced Hg mobilization at the permafrost boundary, due to maximal depth of the thawed peat layer. Both the thickness of the active (unfrozen) peat layer and PHg run-off progressively move to the north during the summer and fall seasons, thus leading to maximal PHg export at the sporadic to discontinuous permafrost zone. The discharge-weighed PHg:POC ratio in western Siberian rivers (2.7±0.5 µg Hg: g C) extrapolated to the whole Ob River basin yields a PHg flux of 1.5±0.3 Mg y^{-1}, consistent with previous estimates. For current climate warming and permafrost thaw scenarios in western Siberia, we predict that a northward shift of permafrost boundaries and increase of active layer depth may enhance the PHg export by rivers to the Arctic Ocean by a factor of two over the next 10-50 years.

1. Introduction

The high-latitude critical zone is subject to changes in hydrological regime (Bring et al., 2016; Wrona et al., 2016) due to widespread permafrost thaw. Climate warming also stimulates organic carbon (OC) release (Vonk et al., 2015), and many trace compounds including toxic mercury (Hg) are tightly linked to OC, both in soils and in river waters (Regnel and Hammar, 2004; Zhang et al., 2015; Kohlenberg et al., 2018; Olson et al., 2018; St. Pierre et al., 2018). Determination of the river Hg flux to the Arctic Ocean has been a topic of active research, since it is of similar magnitude as Hg atmospheric deposition in the Arctic Ocean Hg budget (Amos et al., 2014; Dastoor and Durnford, 2014; Fisher et al., 2012). Sonke et al. (2018) recently constrained a comprehensive pan-arctic river Hg budget that shows equal particulate Hg (PHg) and dissolved (DHg) fluxes to the Arctic Ocean of 22 Mg y^{-1} each. Particulate organic carbon (POC) contributes substantially to the total OC export from continents to the ocean (Schlesinger and Melack, 1981; Lal, 2003; Lamoureux et al., 2014; Galy et al., 2015; Li et al., 2017), and a two-fold increase of Arctic river POC flux by 2100 has been predicted (Gordeev and Kravchishina, 2009).

Consequently, the anticipated increase in POC flux implies that the riverine export of PHg to the coastal zone of the Arctic Ocean may also strongly increase. However, the magnitude of this increase is likely region-specific and depends on a number of environmental parameters such as permafrost coverage, lithology, and the presence of forest, wetlands and lakes in the watershed. Understanding how these parameters affect POC and PHg dynamics is critical for predicting of climate change impacts on Hg transport from the land to the Arctic Ocean.

Despite recent efforts in characterizing PHg fluxes in large Arctic Rivers (Coquery et al., 1995; Amos et al., 2014; Kirk and Louis, 2009; Leitch et al., 2007; Carrie et al., 2012; Quemerais et al., 2009; Sonke et al., 2018), these studies do not identify the factors controlling PHg fluxes in high latitude rivers, which depend on the size of the river watershed and its

landscape (physio-geographical) parameters. In this regard, large continental plains such as the western Siberia Lowland (WSL) which contains huge reservoir of frozen and thawed organic carbon and metals such as Hg (Sheng et al. 2004; Stepanova et al., 2015; Schuster et al., 2018) may be especially useful in assessing environmental controls on PHg export to the Arctic Ocean. Because of the vast amounts of frozen peat with an average thickness of 1 to 3 m, extending over a territory of more than 1 million km², the permafrost thaw in this region can strongly affect the coastal Arctic system via enhanced export of organic-rich river suspended matter (RSM). Due to the homogeneity of the WSL landscape, lithology, and topography, one can use the natural north-south gradient of permafrost zone distribution to assess the direct impact of permafrost conditions on PHg in river waters. The export of Hg by rivers is known to be strongly controlled by organic carbon (Schuster et al., 2011; Kirk et al., 2012; Sonke et al., 2018). In western Siberia, there is a maximum of organic carbon concentration and export fluxes in the sporadic to isolated permafrost zone (Krickov et al., 2018). This zone corresponds to the boundary of permafrost occurrence, and the thawing front of frozen peatlands. We therefore hypothesized a maximum of PHg export by rivers located at the appearance of permafrost (sporadic to isolated zone).

To test this hypothesis and to improve current understanding of magnitude and seasonality of PHg export, we quantified concentrations of PHg across a 1700 km latitudinal gradient with special emphasis on permafrost-bearing zones during three main hydrological periods, the peak of spring flood (early June), the summer base flow (August), and the autumn high flow before the ice on (October). This latitudinal gradient corresponds to that of temperature and permafrost coverage and also reflects the decrease in active layer thickness (ALT) from S to N. We aimed at assessing the effects of latitude (temperature), permafrost coverage and basic landscape features (proportion of bogs, lakes and forest at the watershed) as well as the size of the river watershed on PHg concentration, PHg:POC ratio, and PHg run-off

and flux. Particular attention has been paid to the impact of the size of the river watershed, given that the small rivers are strongly understudied in terms of their suspended load (Holmes et al., 2002). While small rivers allow better assessment of landscape parameters impact on export fluxes, such rivers are hardly accessible in pristine regions, and at the same time, small rivers are often anthropogenically contaminated in populated regions. The WSL allows us to overcome these obstacles due to well-developed road infrastructure in an otherwise pristine region. Finally, we will use our observations to predict changes in PHg fluxes under climate warming, landscape changes and progressive permafrost thaw in the largest frozen peatland province in the world.

2. Study Site and Methods

2.1. Geographical setting

The 32 rivers were sampled in western Siberia Lowland, a large (about 2.6 million km²), peatland and forest zone (**Fig. 1**). The WSL territory encompasses the taiga, forest-tundra and tundra biomes, the positions of which follow the decrease of mean annual air temperature (MAAT) from -0.5°C in the south to -9.5°C in the north. The permafrost distribution also follows the MAAT and changes from absent, isolated and sporadic in the south to discontinuous and continuous in the north. The active layer thickness (ALT) corresponding to the depth of the seasonal thaw of peat layers is equal to 55±10 cm in continuous permafrost zone, 70±20 cm in discontinuous permafrost zone and 160±50 cm in sporadic to isolated zone (Raudina et al., 2017). Further details of WSL physio-geographical settings, peat and lithological description of the territory are provided elsewhere (Kremenetski et al., 2003; Stepanova et al., 2015; Pokrovsky et al., 2015; Raudina et al., 2018) and listed in **Table S1A** of the Supplement. For each biome (taiga, forest-tundra and tundra), several rivers of different watershed size were chosen, following the previous strategy of dissolved WSL river load sampling along the latitudinal transect (Pokrovsky et al., 2015, 2016; Vorobyev et al., 2017). The open water period

lasts about 6 months, from May to October. Most small rivers located within the permafrost zone are frozen during winter period. The 6-months winter discharge is ≤ 10% of annual water flow (Pokrovsky et al., 2015).

2.2. Sampling

Sampling was performed during three main hydrological seasons: spring flood (17 May – 15 June 2016), summer baseflow (1 – 29 August 2016) and autumn baseflow before ice on (24 September – 13 October 2016). During sampling campaigns, we moved from south to north in spring and from north to south in autumn over 2 to 4-weeks period of time, following the natural change of seasons. This allowed to sample all rivers of the transect at approximately the same hydrological stage, after ice off and before ice on. Compared to a 30-year climate record (1985-2015), the year 2016 was normal for western Siberia in terms of spring, summer and autumn precipitation but the temperature was 4 and 2.7°C higher than normal in spring and summer, respectively, and not different from the average temperature in autumn (Rosgidromet, 2017).

Ultraclean sampling and handling was used during river suspended matter (RSM) collection (Krickov et al., 2019). Large volume water samples were taken from the middle of the river at 0.5 m depth in pre-cleaned polypropylene jars (30 to 50 L) from a PVC boat and were decanted during 2 to 3 days to allow the particle settling. The jars were pre-cleaned by detergent, river water, 1 M HCl, MilliQ water, and finally by filling them completely 5 times by river water before collecting the sample for decantation. Some 10% headspace was left in the jars and the lids were not tightened to allow aeration. Note that all river waters sampled in this work were atmospheric oxygen-saturated. As such, the redox conditions in the jars were similar to those of the river water. The jars were protected from daylight to avoid any phytoplankton development and photodegradation of DOM, or photoreduction of Hg. The decantation was done at the river bank, in shadowed areas at the temperature close to that of the river water.

158 During this decantation, the samples were not subjected to biological transformation as
159 particulate organic C, N and P concentrations remained constant and were found to be identical
160 to those determined after immediate filtration and freezing of filters with particulate organic
161 matter (see Krickov et al., 2018 for details). Further, a number of trace metals also demonstrated
162 reasonable agreement in their concentrations in RSM obtained after 2-3 days of decantation and
163 direct filtration (Krickov et al., 2019). Nevertheless, some biogeochemical transformation of
164 PHg bioavailability and speciation during sampling could not be excluded.

165 The water of the bottom layer of the jars (approx. 30% of the initial volume) was
166 centrifuged on-site during 20 min at 3500 rpm using 4 pre-cleaned 50-mL HDPE Nalgene tubes,
167 the particles were recovered on the bottom of these tubes, immediately frozen at -18°C and
168 freeze-dried later in the laboratory. The cleaning of Nalgene tubes for RSM centrifugation,
169 storage and freeze-drying was performed by rinsing with 1N HCl and MilliQ, in a clean room
170 class A 10,000. For determination of RSM bulk concentration, smaller volumes of freshly
171 collected river water (1-2 L) were filtered on-site (at the river bank or in the boat) using pre-
172 weighed acetate cellulose filters (47 mm, 0.45 µm) and Nalgene 250-mL polystyrene filtration
173 units using a Mityvac® manual vacuum pump. This method provided the RSM concentration
174 (mg L^{-1}) which was in reasonable (±10-20%) agreement with the value estimated from total
175 RSM recovery from big jars; see details in Krickov et al. (2018).
176
177 *2.3. Analyses*
178 Total Hg concentration in RSM (PHg_{RSM}, ng g^{-1}) was determined using a direct mercury
179 analyzer (DMA-80 - Milestone, Italy). Total mercury concentration was measured by
180 combustion of the sample at 750 °C, pre-concentration of the Hg^0 vapor released on a gold trap,
181 and detection by atomic absorption. Analysis of reference materials BCR-482 (lichen, 480 ng g^{-1})
182 and MESS-3 (sediment, 91 ng g^{-1}) showed good recoveries of 450±23 ng g^{-1} (n=6, 1σ) and

89±6 ng g^{-1} (n=7, 1σ) respectively. The average uncertainty on duplicate sample analysis did not exceed 5% (1σ). Other measured components included total C and N concentration using catalytic combustion with Cu-O at 900°C with an uncertainty of ≤ 0.5% using Thermo Flash 2000 CN Analyzer at Tomsk University and all major and trace elements. For the latter, the RSM samples were subjected to full acid digestion with bi-distilled HNO_3 and HF in the clean room following ICP-MS (Agilent 7500 ce) analyses as described previously for OC-rich natural samples (Stepanova et al., 2015). The LKSD sediment and 2711a Montana II Soil international standard reference materials (organic-rich sediment and soil) were processed together with RSM samples for quality control (see details in Shevchenko et al., 2017). The Hg_{RSM} (ng g^{-1}) and total RSM concentration in water (mg L^{-1}) allowed calculating PHg concentration in the river water (PHg_{water}, ng L^{-1}).

2.4. Data treatment

In order to assess the specific impact of the permafrost on PHg concentration, we separated all the sampled rivers into five categories: permafrost-free (south of 61°N, 6 rivers), isolated (61 to 63.5°N, 4 rivers); sporadic (63.5 to 65°N, 5 rivers); discontinuous (65 to 66°N, 13 rivers), and continuous permafrost zones (north of 66°N, 4 rivers). Statistical analysis of the RSM chemistry and fluxes in WSL rivers followed the methodology elaborated for particulate C, N and P (Krickov et al., 2018). Because of the non-normal distribution of the PHg_{RSM} and PHg_{water} concentration data, we use median ± interquartile range (IQR) when reporting uncertainty. All statistical tests used a significance level of 5% ($\alpha = 0.05$). The differences in PHg between different seasons and between adjacent permafrost zones were tested using the Mann-Whitney U test for paired data at a significance level of 0.05. For unpaired data, the non-parametric H-criterion Kruskal-Wallis test was performed for all watershed sizes and all permafrost zones. Further, Spearman rank order correlations (significant at $p < 0.05$) were

performed for assessing the effect of latitude, watershed area ($S_{watershed}$), percentage of bogs, forest, lakes at the watershed, the permafrost coverage and bulk concentration of RSM on PHg_{RSM} and PHg_{water}, as well as to characterize the link of PHg with C, N, other major and trace elements. In order to identify the variable(s) responsible for PHg, constrained principal component analysis (PCA) was performed.

The seasonal PHg_{water} export by rivers was calculated separately for spring (May and June), summer (July and August) and autumn (September and October) and integrated for each 2° - wide latitudinal belt of the WSL territory, following the hydrological approach developed for C, major and trace elements (Pokrovsky et al., 2015, 2016). This approach was also used in the recent estimate of particulate C, N and RSM fluxes of WSL rivers (Krickov et al., 2018). Given the small number of measurements for each individual river, the combined uncertainties on these fluxes are estimated as high as ±30%, which stems mainly from uncertainties on water discharges (Pokrovsky et al., 2015; Krickov et al., 2018). However, the integral assessment of riverine export from the WSL territory is robust due to large number of sampled rivers.

Note that there is no direct Hg emission by anthropogenic activity in the studied S-N latitudinal transect of the WSL because there are no industrial centers or coal-fired power plants in the vicinity (50-100 km) of sampling sites. Low Hg contributions from combustion to atmospheric particles is consistent with low concentrations of black carbon in snow collected across the WSL, despite detectable contributions of gas flaring in the northern part of the WSL (Evangeliou et al., 2018).

3. Results

3.1. PHg seasonality and watershed size

Median PHg_{water} concentration in the WSL river waters progressively decreased from the beginning to the end of open water seasons and were equal to 1.7±2.2, 0.9±1.5 and 0.7±1.4 ng L^{-}

233 [1] in spring, summer and autumn, respectively (Table 1). The corresponding Hg_{RSM}
234 concentrations were equal to 237, 124, and 96 ng g^{-1}. Particulate Hg concentrations in individual
235 rivers (**Table S2**) demonstrated that, regardless of watershed area, PHg followed the order
236 spring > summer > autumn. The effect of watershed size on both PHg_{water} and PHg_{RSM} was most
237 pronounced in spring (**Fig. 2A and B**). Although we collected one sample for each river, the
238 sampling was representative of the riverine particles because: 1) we visited all rivers 3 times per
239 year; 2) the sample volume was large (30 to 50 L), and 3) the river water chemical composition
240 in western Siberia is highly stable over full transects of the river channel and on a time scale of 2
241 to 3 days (Vorobyev et al., 2019). The typical RSM concentrations in WSL rivers range from 3
242 to 10 mg L^{-1} with a median value of 7.5 mg L^{-1} (Krickov et al., 2018).
243 Statistical analysis confirmed that PHg_{RSM} depended on watershed area (H= 7.72, p =
244 0.021) in spring whereas both PHg_{RSM} and PHg_{water} depended on watershed area in autumn
245 (H=7.13, p = 0.028; H=8.05, p=0.018, respectively) as shown by the H-criterion of the Kruskal-
246 Wallis test and U-test of Mann-Whitney (**Table S3**). This was also reflected by significant ($p < 0.05$)
247 $R_{Spearman}$ rank order correlations of Hg_{RSM} and size of the watershed (-0.49, -0.39 and -0.45
248 in spring, summer and autumn, respectively, **Table S4**).
249
250 *3.2.Role of landscape parameters and permafrost distribution on PHg*
251 The latitude and permafrost coverage positively correlated with PHg_{RSM} in summer
252 ($R_{Spearman}$ = 0.48 and 0.51, respectively, **Table S4**). The bog coverage exhibited significant ($p < 0.05$)
253 control on PHg_{RSM} which was detectable in spring ($R_{Spearman}$ = 0.56). The effect of forest
254 and lake coverage of watersheds was not significant ($p < 0.05$). There was a peak of both
255 PHg_{water} and PHg_{RSM} in rivers of sporadic permafrost zone in spring (**Fig. 3 A, B**) and a less
256 pronounced maximum of PHg_{water} in rivers of discontinuous permafrost zone in summer (**Fig. 3**
257 **B**). The spring PHg_{RSM} concentrations in absent, isolated and sporadic permafrost zones were ca.

3-5 times higher compared to those in the discontinuous and continuous permafrost zone in spring, whereas the highest PHg_{RSM} were observed in discontinuous and continuous permafrost zones in summer, when PHg_{RSM} was a factor of 2 to 4 higher than in absent, isolated and sporadic permafrost (**Table 1, Fig. 3 B**). Consistent with that, a non-parametric Kruskal-Wallis H-test yielded significant differences in PHg_{water} and PHg_{RSM} among permafrost-free and 4 permafrost-bearing zones in spring (H=15.8, p = 0.0032; H=12.3, p = 0.016, respectively) and autumn (H = 10.2, p = 0.038 for PHg_{water}, **Table S5 A**). The U-test of Mann-Whitney for PHg_{water} and PHg_{RSM} between all adjacent permafrost zones yielded significant differences in spring and for PHg_{water} in autumn ($p < 0.04$, **Table S5 B**). Finally, the Principal Component Analysis (PCA) demonstrated the presence of 3 factors acting on PHg_{water}, PHg_{RSM} and the PHg_{flux} (**Fig. S1** of Supplement). The F1 (30% variance) included latitude, MAAT and permafrost coverage. The F2 (15% variance) comprised the proportion of lakes and forest at the watersheds, C and N. Finally, the F3 (13%) included discharge and the watershed area.

3.3.Correlations of Hg with C, N and other major and trace elements in RSM

There were significant ($p < 0.05$) positive relationships of PHg_{RSM} with OC and N ($R_{Spearman}$ = 0.74 and 0.71, respectively) during spring period. In contrast, negative correlations between PHg_{RSM} and mineral-originated insoluble elements (Al, Ti, Zr, Th, Nb, Ga, Rare Earth Elements ($R_{Spearman}$ = -0.60 to -0.74) were observed (**Table S6**). There was no correlation between PHg_{RSM} and other elements in RSM in summer, whereas in autumn, a number of heavy metals and aerosol-deposited elements demonstrated significant ($p < 0.05$) positive correlation with PHg_{RSM} ($R_{Spearman}$ = 0.41, 0.37, 0.47, 0.43, and 0.59 and 0.42 for Pb, Zn, Cu, Sb, and Mo, respectively).

The Hg:C ratio (µg Hg : g C) in the particulate load of WSL rivers (**Table 1**) was independent of watershed area and generally 3 times higher in spring compared to summer and autumn (**Fig. 4 A**). The Hg:C ratio was similar across all permafrost zones in spring (**Fig. 4 B**). In summer and autumn, the Hg:C ratio was significantly ($p < 0.05$) higher in discontinuous and continuous permafrost zone compared to permafrost-free, isolated and sporadic zones (**Fig. 4 B**). The average discharge-weighted Hg:C ratio in particles of WSL rivers is equal to 2.7±0.5 µg g^{-1} which integrates both permafrost-free and permafrost-bearing zones.

3.4. PHg export flux from the WSL to the Arctic Ocean

An open-water period (May to October) export flux of PHg_{water} across the WSL territory demonstrated a significant ($p < 0.01$, non-parametric Mann-Witney U-test and H-criterion of Kruskal-Wallis) maximum at 61-62°N, in the sporadic permafrost zone (**Fig. 5 A**). In this latitudinal belt, the riverine PHg fluxes were 2.3 and 1.9 times higher than those in permafrost-free and discontinuous/continuous permafrost zones, respectively. The 2-month spring period provided the maximal contribution to open water PHg fluxes in sporadic permafrost zone, whereas the contribution of summer and autumn was the highest in discontinuous and continuous permafrost zone (**Fig. 5 A**). The average PHg export yield from WSL river watersheds during open water period of the year (6 months) ranged from 0.2 to 0.5 g PHg km^{-2} and exhibited a maximum at 61-62°N, within the sporadic permafrost zone (**Table S2, Fig. 5 B**). This zone provided the highest contribution to the overall PHg export flux from permafrost-affected territory of WSL (56 %, **Fig. 5 C**). Note that the winter period contributes less than 10% of RSM, POC and PHg fluxes in Arctic Rivers (McClelland et al., 2016; Sonke et al., 2018). The mean annual air temperature (MAAT), which could be constrained for each permafrost zone but not for individual rivers, shows a maximum in PHg export yield by WSL rivers that corresponds to the sporadic permafrost zone (**Fig. 5 D**). Note that the observed maximum in PHg export was

not linked to latitudinal variation in river runoff. The latter remained fairly constant over full range of studied sites and independent on latitude ($R^2 = 0.08$, **Fig. 5 E**).

4. Discussion

4.1. The influence of watershed size on PHg concentration

The WSL river PHg_{water} concentrations (typically 0.5 to 5.0 ng L^{-1}) are similar to other Arctic rivers of low runoff which drain through boreal zone such as Ob (7.5 ng L^{-1}, Coquery et al., 1995), Severnaya Dvina (4 to 11 ng L^{-1}, Sonke et al., 2018), Yenisey (0.8 to 20 ng L^{-1}, Sonke et al., 2018) and N. American rivers (0.4 to 3.7 ng L^{-1}, Schuster et al., 2011). The PHg_{RSM} values of the WSL rivers (100 to 1000 ng g^{-1}) are in agreement with observations on the Yenisey (60 to 600 ng g^{-1}, Sonke et al., 2018) but higher than N. American rivers (10 to 40 ng g^{-1}, Schuster et al., 2011). A possible reason for high PHg_{RSM} in WSL rivers is high POC concentration, reflecting the dominance of peatlands in Siberian watersheds.

Indeed, small WSL streams ($S_{watershed}$ < 1,000 km²) exhibited significantly higher concentrations of PHg_{RSM} compared to larger rivers (**Fig. 2**). The small streams of WSL have the highest POC concentration in the RSM (Krickov et al., 2018). This suggests enhanced mobilization of PHg in the form of peat debris. Consistently, histosols, the dominant (≥ 50%) soil group of WSL, can provide large amounts of organic particles, given the high susceptibility of peat to physical disintegration compared to mineral sediments (Rezanezhad et al., 2016). The enrichment of the river water in OC-rich particles may occur both at the river banks (especially in small rivers flowing through the wetlands) as well as within extensive floodplains via remobilization of organic-rich sediments at high flow (Krickov et al., 2018; Vorobyev et al., 2019). The floodplains of the Ob river and other rivers of the WSL extend more than 10 times the width of the main channel (Vorobyev et al., 2015). Small rivers also exhibited the largest

scatter in PHg_{RSM} concentrations, probably due to the very short transit time in the watershed, leading to a fast response of river particulate load to minor variations in surface hydrology such as local storm events (e.g., Jeong et al., 2012; Lee et al., 2016).

It is also possible that autochthonous processes of suspended matter transformation in the river channel such as photo- (Mayer et al., 2006; Riggsbee et al., 2008) or bio-degradation (Richardson et al., 2013; Gladyshev et al., 2015; Attermeyer et al., 2018) of particulate organic matter (POM) are capable of modifying PHg_{RSM} to a greater extend in large rivers relative to small streams. The large rivers of WSL have longer water residence times compared to small rivers (Ala-aho et al., 2018a, b). We speculate that, similar to WSL river CO_2 emission (Serikova et al., 2018), the longer travel time of RSM in large rivers may decrease the PHg concentration by biotic or abiotic PHg reduction and evasion of gaseous Hg^0 loss (Gårdfeldt et al., 2001; Poissant et al., 2004; Osterwalder et al., 2017). Overall, the WSL river transport of PHg may be strongly controlled by POM quality and origin, which emphasizes the need to provide molecular-level characterization of POM across permafrost and river-size gradients (McClelland et al., 2016; Kutscher et al., 2017).

The overwhelming role of POM from peat soils as the main factor supplying PHg to rivers is further confirmed by geochemical analyses of RSM and the links of Hg with other elements in the suspended load. Observed negative correlations of PHg_{RSM} with inorganic components of RSM reflect that Hg is bound to organic matter (N, C, $R_{Spearman}$ = 0.79 and 0.76,) and not to the mineral fraction of RSM bearing insoluble (Ti, Al, Zr, REE) silicates, nor to partially soluble carbonate particles containing B, Mg, Ca, Sr, B and U. Therefore, during spring, the mineral fraction of RSM decreases PHg_{RSM} by mere dilution with solid mineral matter. This was especially visible in large rivers, having a higher proportion of silicate minerals in their RSM compared to OC-dominated RSM of small rivers. In autumn, PHg_{RSM} was

positively correlated with Pb, Zn, Cu, Sb, and Mo which could reflect co-deposition from the atmospheric dust to vegetation and soils (Shevchenko et al., 2017).

4.2. Impact of permafrost coverage on PHg

Climate and permafrost coverage are considered as main drivers of dissolved and particulate river load in the WSL (Frey et al., 2007; Frey and Smith, 2005; Pokrovsky et al., 2015). Due to very flat topography of this region, the permafrost distribution in western Siberia roughly follows the latitude and MAAT so that there is a progressive change of the permafrost zones ("absent → isolated → sporadic → discontinuous → continuous") in the south → north direction. Both PHg_{water} and PHg_{RSM} demonstrated a maximum around 60-62°N, in the sporadic and discontinuous permafrost zones (**Fig. 3**). The May-October PHg export fluxes were also maximal in this part of the WSL (**Fig. 5 B, C**). Note that spatial patterns of PHg fluxes in western Siberia cannot be explained by latitudinal variation of precipitation or runoff, because the water runoff remains constant or gradually increases northward (Pokrovsky et al., 2015 and **Fig. 5 E**).

The discontinuous permafrost zone can be considered as a large-scale thawing front of the frozen peat, and corresponds to the southern boundary of permafrost persistence. Here, an enhanced mobilization of C- and N-rich particles from soils to rivers (Krickov et al., 2018) and maximal CO_2 emission from rivers (Serikova et al., 2018) occur. Further, a maximum of PHg_{RSM} and export fluxes occurred in isolated and sporadic permafrost in spring. This maximum shifted to discontinuous permafrost zone in summer and moved northward, to the discontinuous permafrost zone in autumn (**Fig. 3 B and 5 A**, respectively).

The active (unfrozen) layer thickness increases from spring to autumn and more importantly it moves northward during the open –water period from May to October (Trofimova and Balybina, 2014; Raudina et al., 2017). This increase controls the degree of peat and mineral particles eroding from the soil profile to the rivers (e.g., Krickov et al., 2018). Thus, enhanced mobilization and subsequent river inputs of C, nutrients and metals at the "hot spot" of the permafrost thawing front was reported at the local scale of frozen peat landscapes of western Siberia (Loiko et al., 2017).

The 2 to 3 times higher Hg:C ratio in spring compared to summer and autumn likely reflects the run-off of snow Hg that accumulated by atmospheric deposition over the previous 6 months cold season. The Hg:C ratio in RSM during summer and autumn was 2 to 3 times higher in northern rivers of discontinuous and continuous permafrost zone compared to southern rivers (**Fig. 4 B**). Note that during this period, the water travel times in the WSL rivers and from the soil profile to the river are much shorter in the north than in the south (Ala-aho et al., 2018b).

We hypothesize that the breakdown of river POM to CO_2 (Serikova et al., 2018; Krickov et al., 2018) leads to concomitant reduction and volatilization of PHg. This process is then more pronounced in the southern rivers with longer water residence time, while in the north, more refractory organic matter of RSM (Gladyshev et al., 2015) and lower biological activity (Kawahigashi et al., 2004) lead to better preservation of POM-bound Hg in riverine particles. This may produce the observed Hg to C enrichment in the RSM of northern rivers during the summer and fall base flow period.

Overall, PHg generation in WSL rivers across the permafrost gradient may depend on both the PHg supply and losses in the catchments. Atmospheric Hg retention in continental ecosystems is thought to be dominated by the plant Hg pump during the vegetation growth season, where vegetation directly sequesters gaseous elemental Hg^0 from the atmosphere (Obrist et al., 2017; Jiskra et al., 2018). During the winter season Hg deposition is likely dominated by

wet deposition in the form of snowfall (Nelson et al., 2010). The main sources of suspended matter in WSL rivers are 1) vegetation litter such as plant leaves in the south and mosses, lichens and dwarf shrub leafs in the permafrost-bearing zone; these organic debris are easily mobilized by surface run-off to the river, notably in spring during snow melt; 2) surface and deep peat and mineral horizons, providing the particles via bank abrasion in spring and via supra-permafrost flow in summer and autumn, and 3) lake and bog open water sediments as well as flood plain sediments. In the north, soil erosion is limited by the low thickness (30-40 cm) of the active (unfrozen) layer and the low net primary productivity, providing POM, whereas in the south, the soil is stabilized by abundant forest vegetation. We suggest that in the north, shallow unfrozen peat depth and lower biomass accumulation cannot supply sufficiently high PHg and the fluxes remain relatively low in spring. In contrast, the PHg concentration and fluxes greatly increase in summer, when the thickness of active (unfrozen) peat layer increases in the north. As such, physical erosion of peat soils in the WSL drives maximum RSM levels at the sporadic permafrost zone due to maximal thickness of unfrozen histosols, notably in the beginning of the snow-free season.

4.3. PHg flux and climate warming in western Siberia

The Taz and Pur Rivers ($S_{watershed}$ = 150,000 and 112,000 km²) integrate a significant part of permafrost-affected WSL territory, and export ca. 0.036 and 0.0067 Mg PHg y^{-1} (Table 1). The PHg flux of these two rivers represents less than 0.4 % of the overall Eurasian River (S_{total} = 10,962,000 km²) flux (11.3 Mg PHg y^{-1}, Sonke et al., 2018) which is disproportionally (6.5 times) low compared to their total watershed area and respective discharge. The most likely cause for this is low concentration and low annual yield of RSM in WSL rivers due to low water runoff (100-200 mm y^{-1}) and limited river slopes. Measured open-water period PHg export

yields of Ob, Pur and Taz (0.20, 0.06, and 0.24 g km^{-2} y^{-1}, respectively, **Table S2**) are lower than the modeled yields by Sonke et al. (2018) (0.63, 1.5 and 1.7 g km^{-2} y^{-1}, respectively).

It is possible that the individual PHg fluxes of WSL rivers, assessed in this study, are biased by small number of sampling days, and poor constraining of water discharges for these essentially ungauged rivers. However, the Hg:C ratio, which is based on a large number of measurements, may become an efficient proxy for reconstructing overall Hg export based on known POC export. Indeed, the measured PHg and POC fluxes of Arctic Rivers (Leitch et al., 2007; Kirk et al., 2009; Carrie et al., 2012; Sonke et al., 2018; McClelland et al., 2016) yield ranges of Hg:C (Mg:Tg) ratios equal to 2.0-4.8 (MacKenzie), 1.3-2.8 (Sev. Dvina), and 2.6-7.8 (Yenisey). This is consistent with the discharge-weighted Hg:C ratio of 2.7±0.5 recommended for WSL rivers in this study. Further, using the mean ratio Hg:C of open water time period in rivers of WSL, and overall POC flux of the pan-Arctic rivers (5.77 Tg y^{-1}, McClelland et al., 2016), the pan-Arctic flux of PHg is equal to 15.6±3.0 Mg y^{-1} which is comparable to the value 21.9 Mg y^{-1}, assessed by Sonke et al (2018). For the Ob River with its 0.57 Tg POC y^{-1} flux (McClelland et al., 2016), the observation-based PHg flux is 1.5±0.3 Mg PHg y^{-1} in this study, in agreement with 1.4 Mg PHg y^{-1} modeled by Sonke et al. (2018) based on Hg-DOC and Hg-discharge relationships.

Our results allow a first order assessment of the consequences of climate warming and permafrost thaw in western Siberia on riverine transport of PHg from the land to the Arctic Ocean. For this, we can employ a "substituting space for time" approach which was successfully used in western Siberia for the dissolved (< 0.45 µm) fraction of inorganic river loads (Frey et al., 2007), DOC (Frey and Smith, 2005; Pokrovsky et al., 2015), trace metals (Pokrovsky et al., 2016), nutrients (Vorobyev et al., 2017), as well as CO_2 emission scenarios (Serikova et al., 2018). In a broader context, the "space-for-time" substitution approach postulates that

453 contemporary spatial phenomena can be used to understand and model temporal processes that
454 are otherwise unobservable, such as past and future events (Blois et al., 2013).

455 In the northern part of the WSL, soil temperature may rise by 0.15 to 0.3 degree per 10
456 years over next 50 to 100 years (Pavlov et al., 2009; Anisimov et al., 2012). On a short-term
457 prospective (10-50 years), this will transform the discontinuous and continuous permafrost zones
458 into sporadic and isolated permafrost (Anisimov and Reneva, 2006). Given the current
459 maximum of PHg at the sporadic PF zone, this may enhance both concentrations and fluxes of
460 PHg in the northern rivers, roughly by a factor of 2 (see **Figs 3 and 5B**), which will also enhance
461 the export of PHg to the Arctic Ocean. On a longer prospective (50-150 years), the
462 discontinuous and continuous permafrost may disappear (Romanovsky et al., 2008; Nadyozhina
463 et al., 2008) and the border of isolated to sporadic permafrost development will follow the Arctic
464 circle (Bedritsky et al., 2018). Moreover, if the current rate of soil warming persists, by 2100,
465 the active layer thickness may reach 4 m in the tundra of Yamal Peninsula which is currently
466 continuous permafrost zone (Sudakov et al., 2011). These changes will certainly produce much
467 deeper water paths in organic and mineral soils. Progressive moving of the permafrost thawing
468 front to the north will therefore locally and temporarily increase PHg concentration and fluxes at
469 the sites of maximal ALT. However, complete disappearance of permafrost in the north of WSL
470 may bring about a decrease in PHg export by northern rivers to the values which are currently
471 observed in rivers south of 60°N. Furthermore, if the permafrost-free zone expands northward
472 into the current sporadic zone, this could produce a concomitant reduction in PHg fluxes thus
473 compensating for the shift northwards of the sporadic zone.
474

475 **Conclusions**

476 The concentration of particulate Hg (PHg) in the WSL rivers is controlled by the organic
477 nature of abundant peat soils that dominate river watersheds. The overwhelming role of deep

478 and intermediate peat horizons rather than mineral layers, surface peat and plant litter in
479 providing Hg to riverine suspended load is confirmed by *i*) strong positive correlation between
480 C, N and Hg in RSM, and *ii*) much higher PHg_{RSM} and PHg_{water} in discontinuous and sporadic
481 permafrost rivers compared to southern, permafrost–free or northern, continuous permafrost–
482 bearing rivers.

483 The concentration of Hg in RSM decreased with the increase in river watershed size,
484 illustrating the importance of organic particles in small rivers which drain peatlands and the
485 abundance of mineral matter from bank abrasion in larger rivers. This was most visible in
486 spring, when the bank abrasion and sediment transport and deposition within the floodplains
487 were pronounced. Overall, the spring flood provided the largest contribution to overall PHg
488 export by WSL rivers to the Arctic Ocean, despite its relatively short duration (2 of 6 months of
489 open-water period).

490 At the sporadic permafrost zone, we observed maximum concentration and export fluxes
491 of PHg, which corresponded to peak of particulate C and N concentration and fluxes across the
492 latitudinal profile. This suggests the enhanced generation of Hg, C-rich RSM at the thawing
493 front of permafrost, where the thickness of the active layer is maximal.

494 To assess a northward permafrost boundary shifts with increases in air and soil
495 temperature we used a substituting space for time scenario of climate warming in the WSL, well
496 developed for the dissolved fraction of C and metals. From a short-term (10-50 years) climate
497 warming perspective, the effect of a simple northward shift of permafrost boundary may produce
498 a two-fold increase in PHg concentration and fluxes in rivers of the discontinuous and
499 continuous permafrost zone. On longer time scales (50-100 years), full disappearance of
500 permafrost in the northern part of WSL may decrease the concentrations of PHg in the river
501 water and its export fluxes back to their contemporary level.
502

Acknowledgements:

This work was supported by RSCF No 18-17-00237 “Mechanisms of hydrochemical runoff of the Ob river flood zone” (analyses, modeling); RFBR projects № 18-35-00563\18 and 19-55-15002; the TSU competitiveness improvement programme Project No 8.1.04.2018, the Ministry of Education and Science of the Russian Federation No. 1.8195.2017/P220, the CNRS Chantier Arctique, via the PARCS project, and the H2020 ERA-PLANET (689443) iGOSP and iCUPE programmes.

References

Ala-Aho, P., Soulsby, C., Pokrovsky, O.S., Kirpotin, S.N., S.N., Karlsson, J., Serikova, S., Manasypov, R.M., Krickov, I., Lim, A., Tetzlaff, D., 2018a. Permafrost and lakes control river isotope composition across a boreal-arctic transect in the western Siberia lowland. Environ. Res. Lett. 13 (3), 034028. https://doi.org/10.1088/1748-9326/aaa4fe.

Ala-Aho, P., Soulsby, C., Pokrovsky, O.S., Kirpotin, S.N., Karlsson, J., Serikova, S., Vorobyev, S.N., Manasypov, R.M., Loiko, S., Tetzlaff, D., 2018b. Using stable isotopes to assess surface water source dynamics and hydrological connectivity in a high-latitude wetland and permafrost influenced landscape. J. Hydrol. 556, 279–293. https://doi.org/10.1016/j.jhydrol.2017.11.024.

Amos, H. M., Jacob, D. J., Kocman, D., Horowitz, H. M., Zhang, Y., Dutkiewicz, S., Horvat, M., Corbitt, E. S., Krabbenhoft, D. P., Sunderland, E. M., 2014. Global biogeochemical implications of mercury discharges from rivers and sediment burial. Environ. Sci. Technol. 48(16), 9514-9522. https://doi.org/10.1021/es502134t.

Anisimov, O. A., Anokhin, A., Lavrov, S. A., Malkova, G. V., Pavlov, A. V., Romanovskiy, V. E., Streletskiy, D. A., Kholodov, A. L., Shiklomanov, N. I., 2012. Continental multiyear permafrost, in: Semenov, S.M. (Eds.), Methods of study the sequences of climate changes for nature systems. VNIIGMI, Moscow, pp. 268–328. (In Russian)

Anisimov, O., Reneva, S., 2006. Permafrost and changing climate: the Russian perspective. AMBIO: A Journal of the Human Environment 35(4), 169-176. https://doi.org/10.1579/0044-7447(2006)35[169:PACCTR]2.0.CO;2.

Attermeyer, K., Catalán, N., Einarsdottir, K., Freixa, A., Groeneveld, M., Hawkes, J. A., Bergquist, J., Tranvik, L. J., 2018. Organic carbon processing during transport through boreal inland waters: Particles as important sites. J. Geophys. Res.-Biogeo. 123(8), 2412-2428. https://doi.org/10.1029/2018JG004500.

Bedritsky A. I., 2018. National report “Global climate and soil cover f Russia: estimation of risks and environmental and econoical consequences of land degradation. Adaptive systems and technologies of agriculture and forestry”, GEOS, Moscow.

Blois, J. L., Williams, J. W., Fitzpatrick, M. C., Jackson, S. T., Ferrier, S., 2013. Space can substitute for time in predicting climate-change effects on biodiversity. Proc. Natl. Acad. Sci. U. S. A. 110 (23), 9374-9379. https://doi.org/10.1073/pnas.1220228110.

Bring, A., Fedorova, I., Dibike, Y., Hinzman, L., Mård, J., Mernild, S. H., Prowse, T., Semenova, O., Stuefer, S. L., Woo, M. K., 2016. Arctic terrestrial hydrology: A synthesis of processes, regional effects, and research challenges. J. Geophys. Res.-Biogeo. 121(3), 621-649. http://dx.doi.org/10.1002/2015JG003131.

Carrie, J., Stern, G. A., Sanei, H., Macdonald, R. W., Wang, F., 2012. Determination of mercury biogeochemical fluxes in the remote Mackenzie River Basin, northwest Canada, using

549 speciation of sulfur and organic carbon. Appl. Geochem. 27(4), 815-824.
550 https://doi.org/10.1016/j.apgeochem.2012.01.018.
551 Coquery, M., Cossa, D., Martin, J. M., 1995. The distribution of dissolved and particulate mercury
552 in three Siberian estuaries and adjacent Arctic coastal waters. Water, Air, and Soil Pollution
553 80(1-4), 653-664.
554 Dastoor, A., Durnford, D. 2014. Arctic Ocean: Is it a sink or a source of atmospheric mercury?,
555 Environ. Sci. Technol., 48(3), 1707–1717, doi:10.1021/es404473e.
556 Evangeliou, N., Shevchenko, V. P., Yttri, K.-E., Eckhardt, S., Sollum E., Pokrovsky, O. S.,
557 Kobelev, V. O., Korobov, V. B., Lobanov, A. A., Starodymova, D. P., Vorobiev, S. N.,
558 Thompson, R. L., Stohl, A., 2018. Origin of elemental carbon in snow from western Siberia
559 and northwestern European Russia during winter–spring 2014, 2015 and 2016. Atmos. Chem.
560 Phys. 18(2), 963-977. https://doi.org/10.5194/acp-18-963-2018.
561 Fisher, J. A., Jacob, D. J., Soerensen, A. L., Amos, H. M., Steffen, A., Sunderland, E. M., 2012.
562 Riverine source of Arctic Ocean mercury inferred from atmospheric observations. Nat.
563 Geosci. 5(7), 499-504. http://www.nature.com/doifinder/10.1038/ngeo1478.
564 Frey, K. E., Siegel, D. I., Smith, L. C., 2007. Geochemistry of west Siberian streams and their
565 potential response to permafrost degradation. Water resources research 43(3), W03406.
566 https://doi.org/10.1029/2006WR004902.
567 Frey, K. E., Smith, L. C., 2005. Amplified carbon release from vast West Siberian peatlands by
568 2100. Geophys. Res. Lett. 32(9), L09401. https://doi.org/10.1029/2004GL022025.
569 Galy, V., Peucker-Ehrenbrink, B., Eglinton, T., 2015. Global carbon export from the terrestrial
570 biosphere controlled by erosion. Nature 521(7551), 204.
571 http://dx.doi.org/10.1038/nature14400.
572 Gladyshev, M. I., Kolmakova, O. V., Tolomeev, A. P., Anishchenko, O. V., Makhutova, O. N.,
573 Kolmakova, A. A., Kravchuk, E. S., Glushchenko, L. A., Kolmakov, V. I., Sushchik, N. N.,
574 2015. Differences in organic matter and bacterioplankton between sections of the largest
575 Arctic river: Mosaic or continuum?. Limnol. Oceanogr. 60(4), 1314-1331.
576 https://doi.org/10.1002/lno.10097.
577 Gårdfeldt, K., Feng, X., Sommar, J., Lindqvist, O., 2001. Total gaseous mercury exchange between
578 air and water at river and sea surfaces in Swedish coastal regions. Atmos. Environ. 35(17),
579 3027-3038. https://doi.org/10.1016/S1352-2310(01)00106-6
580 Gordeev, V. V., Martin, J. M., Sidorov, I. S., Sidorova, M. V., 1996. A reassessment of the
581 Eurasian river input of water, sediment, major elements, and nutrients to the Arctic Ocean.
582 Am. J. Sci. 296(6), 664-691. https://doi.org/10.2475/ajs.296.6.664.
583 Gordeev, V. V., Kravchishina, M. D., 2009. River flux of dissolved organic carbon (DOC) and
584 particulate organic carbon (POC) to the Arctic Ocean: what are the consequences of the
585 global changes?, in: Nihouls, J. C. J., Kostianoy, A. G. (Eds.), Influence of Climate Change
586 on Changing Arctic and Sub-Arctic Conditions. Springer, Dordrecht, pp. 145-160.
587 Jeong, J. J., Bartsch, S., Fleckenstein, J. H., Matzner, E., Tenhunen, J. D., Lee, S. D., Park, S. K.,
588 Park, J. H., 2012. Differential storm responses of dissolved and particulate organic carbon
589 in a mountainous headwater stream, investigated by high-frequency, in situ optical
590 measurements. J. Geophys. Res.-Biogeo. 117, G03013.
591 https://doi.org/10.1029/2012JG001999.
592 Jiskra, M., Sonke, J. E., Obrist, D., Bieser, J., Ebinghaus, R., Myhre, C. L., Pfaffhuber, K. A.,
593 Wängberg, I., Kyllönen, K., Worthy, D., Martin, L. G., Labuschagne, C., Mkololo, T.,
594 Ramonet, M., Magand, O., Dommergue, A., 2018. A vegetation control on seasonal
595 variations in global atmospheric mercury concentrations. Nat. Geosci. 11(4), 244.
596 https://doi.org/10.1038/s41561-018-0078-8.

Kawahigashi, M., Kaiser, K., Kalbitz, K., Rodionov, A., Guggenberger, G., 2004. Dissolved organic matter in small streams along a gradient from discontinuous to continuous permafrost. Glob. Change Biol. 10(9), 1576-1586. https://doi.org/10.1111/j.1365-2486.2004.00827.x.

Kirk, J. L., St. Louis, V. L., 2009. Multiyear total and methyl mercury exports from two major sub-Arctic rivers draining into Hudson Bay, Canada. Environ. Sci. Technol. 43(7), 2254-2261. https://doi.org/10.1021/es803138z.

Kirk, J. L., Lehnherr, I., Andersson, M., Braune, B. M., Chan, L., Dastoor, A. P., Durnford, D., Gleason., A. L., Loseto, L. L., Steffen, A., St. Louisj, V. L., 2012. Mercury in Arctic marine ecosystems: Sources, pathways and exposure. Environ. Res. 119, 64-87. https://doi.org/10.1016/j.envres.2012.08.012.

Kohlenberg, A. J., Turetsky, M. R., Thompson, D. K., Branfireun, B. A., Mitchell, C. P., 2018. Controls on boreal peat combustion and resulting emissions of carbon and mercury. Environ. Res. Lett. 13(3), 035005. https://doi.org/10.1088/1748-9326/aa9ea8.

Kremenetski, K. V., Velichko, A. A., Borisova, O. K., MacDonald, G. M., Smith, L. C., Frey, K. E., Orlova, L. A., 2003. Peatlands of the Western Siberian lowlands: current knowledge on zonation, carbon content and Late Quaternary history. Quaternary Sci. Rev. 22(5-7), 703-723. https://doi.org/10.1016/S0277-3791(02)00196-8.

Krickov, I. V., Lim, A. G., Manasypov, R. M., Loiko, S. V., Shirokova, L. S., Kirpotin, S. N., Karlsson, J., Pokrovsky, O. S., 2018. Riverine particulate C and N generated at the permafrost thaw front: case study of western Siberian rivers across a 1700km latitudinal transect. Biogeosciences 15(22), 6867-6884. https://doi.org/10.5194/bg-15-6867-2018.

Krickov, I. V., Lim, A. G., Loiko, S. V., Manasypov, R. M., Vorobyev, S. N., Shevchenko, V. P., Gordeev, V. V., Pokrovsky, O. S., 2019. Major and trace elements in suspended matter of western Siberian rivers: first assessment across permafrost zones and landscape parameters of watersheds. Geochim. Cosmochim. Acta, submitted after revision.

Klaminder, J., Yoo, K., Rydberg, J., Giesler, R., 2008. An explorative study of mercury export from a thawing palsa mire. J. Geophys. Res.-Biogeo. 113(G4). https://doi.org/10.1029/2008JG000776.

Kutscher, L., Mörth, C. M., Porcelli, D., Hirst, C., Maximov, T. C., Petrov, R. E., Andersson, P. S., 2017. Spatial variation in concentration and sources of organic carbon in the Lena River, Siberia. J. Geophys. Res.-Biogeo. 122(8), 1999-2016. https://doi.org/10.1002/2017JG003858.

Lal, R., 2003. Soil erosion and the global carbon budget. Environ. Int. 29(4), 437-450. https://doi.org/10.1016/S0160-4120(02)00192-7.

Lamoureux, S. F., Lafrenière, M. J., 2014. Seasonal fluxes and age of particulate organic carbon exported from Arctic catchments impacted by localized permafrost slope disturbances. Environ. Res. Lett. 9(4), 045002. http://dx.doi.org/10.1088/1748-9326/9/4/045002.

Lee, M. H., Payeur-Poirier, J. L., Park, J. H., Matzner, E., 2016. Variability in runoff fluxes of dissolved and particulate carbon and nitrogen from two watersheds of different tree species during intense storm events. Biogeosciences 13(18), 5421. http://dx.doi.org/10.5194/bg-13-5421-2016.

Leitch, D. R., Carrie, J., Lean, D., Macdonald, R. W., Stern, G. A., Wang, F., 2007. The delivery of mercury to the Beaufort Sea of the Arctic Ocean by the Mackenzie River. Sci. Total Environ. 373(1), 178-195. https://doi.org/10.1016/j.scitotenv.2006.10.041.

Li, M., Peng, C., Wang, M., Xue, W., Zhang, K., Wang, K., Shi, G., Zhu, Q., 2017. The carbon flux of global rivers: a re-evaluation of amount and spatial patterns. Ecol. Indic. 80, 40-51. https://doi.org/10.1016/j.ecolind.2017.04.049.

Loiko, S. V., Pokrovsky, O. S., Raudina, T. V., Lim, A., Kolesnichenko, L. G., Shirokova, L. S., Vorobyev, S. N., Kirpotin, S. N., 2017. Abrupt permafrost collapse enhances organic carbon, CO2, nutrient and metal release into surface waters. Chem. Geol. 471, 153-165. https://doi.org/10.1016/j.chemgeo.2017.10.002.

Mayer, L. M., Schick, L. L., Skorko, K., Boss, E., 2006. Photodissolution of particulate organic matter from sediments. Limnol. Oceanogr. 51(2), 1064-1071.

McClelland, J. W., Holmes, R. M., Peterson, B. J., Raymond, P. A., Striegl, R. G., Zhulidov, A. V., Zimov, S. A., Zimov, N., Tank, S. E., Spencer, R. G. M., Staples, R., Gurtovaya, T. Y., Griffin, C. G., 2016. Particulate organic carbon and nitrogen export from major Arctic rivers. Global Biogeochem. Cy. 30(5), 629-643. https://doi.org/10.1002/2015GB005351.

Nadyozhina, E. D., Shkolnik, I. M., Pavlova, T. V., Molkentin, E. K., Semioshina, A. A., 2008. Permafrost response to the climate warming as simulated by the regional climate model of the main geophysical observatory. Earth's Cryosphere 12(3), 3-11. (In Russian).

Nelson, S. J., Fernandez, I. J., Kahl, J. S., 2010. A review of mercury concentration and deposition in snow in eastern temperate North America. Hydrol. Processes, 24, 1971-1980.

Obrist, D., Agnan, Y., Jiskra, M., Olson, C. L., Colegrove, D. P., Hueber, J., Moore, C. W., Sonke, J. E., Helmig, D., 2017. Tundra uptake of atmospheric elemental mercury drives Arctic mercury pollution. Nature 547(7662), 201. https://doi.org/10.1038/nature22997.

Olson, C., Jiskra, M., Biester, H., Chow, J., Obrist, D., 2018. Mercury in Active-Layer Tundra Soils of Alaska: Concentrations, Pools, Origins, and Spatial Distribution. Global Biogeochem. Cy. 32(7), 1058-1073. https://doi.org/10.1029/2017GB005840.

Osterwalder, S., Bishop, K., Alewell, C., Fritsche, J., Laudon, H., Akerblom, S., Nilsson, M. B., 2017. Mercury evasion from a boreal peatland shortens the timeline for recovery from legacy pollution. Sci. Rep., 7, Art No 16022.

Pavlov, A. V., Malkova, G. V., 2009. Small-scale mapping of trends of the contemporary ground temperature changes in the Russian North. Earth's Cryosphere 13(4), 32-39.

Poissant, L., Pilote, M., Constant, P., Beauvais, C., Zhang, H. H., Xu, X., 2004. Mercury gas exchanges over selected bare soil and flooded sites in the bay St. Francois wetlands (Quebec, Canada). Atmos. Environ. 38(25), 4205-4214. https://doi.org/10.1016/j.atmosenv.2004.03.068

Pokrovsky, O. S., Manasypov, R. M., Loiko, S., Shirokova, L. S., Krickov, I. A., Pokrovsky B. G., Kolesnichenko, L. G., Kopysov, S. G., Zemtzov, V. A., Kulizhsky, S. P., Vorobyev, S. N., Kirpotin, S. N., 2015. Permafrost coverage, watershed area and season control of dissolved carbon and major elements in western Siberian rivers. Biogeosciences 12, 6301–6320. https://doi.org/10.5194/bg-12-6301-2015.

Pokrovsky, O. S., Manasypov, R. M., Loiko, S. V., Krickov, I. A., Kopysov, S. G., Kolesnichenko, L. G., Vorobyev, S. N., Kirpotin, S. N., 2016. Trace element transport in western Siberian rivers across a permafrost gradient. Biogeosciences 13(6), 1877-1900. https://doi.org/10.5194/bg-13-1877-2016.

Quémerais, B., Cossa, D., Rondeau, B., Pham, T. T., Gagnon, P., 1999. Sources and fluxes of mercury in the St. Lawrence River. Environ. Sci. Technol. 33(6), 840-849. https://doi.org/10.1021/es980400a.

Raudina, T. V., Loiko, S. V., Lim, A. G., Krickov, I. V., Shirokova, L. S., Istigechev, G. I., Kuzmina, D. M., Kulizhsky, S. P., Vorobyev, S. N., Pokrovsky, O. S., 2017. Dissolved organic carbon and major and trace elements in peat porewater of sporadic, discontinuous, and continuous permafrost zones of western Siberia. Biogeosciences 14(14), 3561-3584. https://doi.org/10.5194/bg-14-3561-2017.

Raudina, T. V., Loiko, S. V., Lim, A., Manasypov, R. M., Shirokova, L. S., Istigechev, G. I., Kuzmina, D. M., Kulizhsky, S. P., Vorobyev, S. N., Pokrovsky, O. S., 2018. Permafrost thaw and climate warming may decrease the CO2, carbon, and metal concentration in peat soil waters of the Western Siberia Lowland. Sci. Total Environ. 634, 1004-1023. https://doi.org/10.1016/j.scitotenv.2018.04.059.

Rosgidromet, R. F., 2017. A report on climate features on the territory of the Russian federation in 2016, Moscow. (in Russian).

Regnell, O., Hammar, T., 2004. Coupling of methyl and total mercury in a minerotrophic peat bog in southeastern Sweden. Can. J. Fish. Aquat. Sci. 61(10), 2014-2023. https://doi.org/10.1139/f04-143.

Rezanezhad, F., Price, J. S., Quinton, W. L., Lennartz, B., Milojevic, T., Van Cappellen, P., 2016. Structure of peat soils and implications for water storage, flow and solute transport: A review update for geochemists. Chem. Geol., 429, 75-84.

Richardson, D. C., Newbold, J. D., Aufdenkampe, A. K., Taylor, P. G., Kaplan, L. A., 2013. Measuring heterotrophic respiration rates of suspended particulate organic carbon from stream ecosystems. Limnol. Oceanogr.-Meth. 11(5), 247-261. https://doi.org/10.4319/lom.2013.11.247.

Riggsbee, J. A., Orr, C. H., Leech, D. M., Doyle, M. W., Wetzel, R. G., 2008. Suspended sediments in river ecosystems: Photochemical sources of dissolved organic carbon, dissolved organic nitrogen, and adsorptive removal of dissolved iron. J. Geophys. Res.-Biogeo. 113(G3). https://doi.org/10.1029/2007JG000654.

Romanovsky, V. E., Kholodov, A. L., Marchenko, S. S., Oberman, N. G., Drozdov, D. S., Malkova, G. V., Moskalenko, N. G., Vasiliev, A. A., Sergeev, D. O., Zheleznyak, M. N., 2008. Thermal state and fate of permafrost in Russia: first results of IPY, in: Kane, D. L., Hinkel, K. M. (Eds.), Ninth International Conference on Permafrost, University of Alaska, Fairbanks, pp. 1511-1518.

Serikova, S., Pokrovsky, O. S., Ala-Aho, P., Kazantsev, V., Kirpotin, S. N., Kopysov, S. G., Krickov, I. V., Laudon, H., Manasypov, R. M., Shirokova, L. S., Soulsby, C., Tetzlaff, D., Karlsson, J., 2018. High riverine CO_2 emissions at the permafrost boundary of Western Siberia. Nat. Geosci. 11, 825. https://doi.org/10.1038/s41561-018-0218-1.

Sheng, Y., Smith, L. C., MacDonald, G. M., Kremenetski, K. V., Frey, K. E., Velichko, A. A., Lee, V., Beilman, W. B., Dubinin, P., 2004. A high-resolution GIS-based inventory of the west Siberian peat carbon pool. Global Biogeochem. Cy. 18(3). https://doi.org/10.1029/2003GB002190.

Shevchenko, V. P., Pokrovsky, O. S., Vorobyev, S. N., Krickov, I. V., Manasypov, R. M., Politova, N. V., Kopysov, S. G., Dara, O. M., Auda, Y., Shirokova, L. S., Kolesnichenko, L. G., Zemtsov, V. A., Kirpotin, S. N., 2017. Impact of snow deposition on major and trace element concentrations and elementary fluxes in surface waters of the Western Siberian Lowland across a 1700 km latitudinal gradient. Hydrol. Earth Syst. Sc. 21(11), 5725-5746. https://doi.org/10.5194/hess-21-5725-2017.

Schlesinger, W. H., Melack, J. M., 1981. Transport of organic carbon in the world's rivers. Tellus 33(2), 172-187. https://doi.org/10.3402/tellusa.v33i2.10706.

Schuster, P. F., Striegl, R. G., Aiken, G. R., Krabbenhoft, D. P., Dewild, J. F., Butler, K., Kamark, B., Dornblaser, M., 2011. Mercury export from the Yukon River Basin and potential response to a changing climate. Environ. Sci. Technol. 45(21), 9262-9267. https://doi.org/10.1021/es202068b.

Schuster, P. F., Schaefer, K. M., Aiken, G. R., Antweiler, R. C., Dewild, J. F., Gryziec, J. D., Gusmeroli, A., Hugelius, G., Jafarov, E., Krabbenhoft, D. P., Liu, L., Herman-Mercer, N., Mu, C., Roth, D. A., Schaefer, T., Striegl, R. G., Wickland, K. P., Zhang, T., 2018. Permafrost stores a globally significant amount of mercury. Geophys. Res. Lett. 45(3), 1463-1471. http://dx.doi.org/10.1002/2017GL075571.

St. Pierre, K. A., Zolkos, S., Shakil, S., Tank, S. E., St. Louis, V. L., Kokelj, S. V., 2018. Unprecedented increases in total and methyl mercury concentrations downstream of retrogressive thaw slumps in the western Canadian Arctic. Environ. Sci. Technol. 52(24), 14099-14109. https://doi.org/10.1021/acs.est.8b05348.

Sonke, J. E., Teisserenc, R., Heimbürger-Boavida, L. E., Petrova, M. V., Marusczak, N., Le Dantec, T., Chupakov, A. V., Li, C., Thackray, C. P., Sunderland, E. M., Tananaev, N.,

Pokrovsky, O. S., 2018. Eurasian river spring flood observations support net Arctic Ocean mercury export to the atmosphere and Atlantic Ocean. P. Natl. Acad. Sci. USA 115(50), E11586-E11594. https://doi.org/10.1073/pnas.1811957115.

~~Soerensen, A., Jacob, J.D., Schartup, A., Fisher, A., Lehnherr J., St.Louis, V., Heimbürger-Boavida, L-E., Sonke, J.E., Krabbenhoft, D., Sunderland, E., 2016. A Mass Budget for Mercury and Methylmercury in the Arctic Ocean. Global Biogeochemical Cycles, 30, 10.1002/2015GB005280, DOI: 10.1002/2015GB005280~~

Stepanova, V. M., Pokrovsky, O. S., Viers, J., Mironycheva-Tokareva, N. P., Kosykh, N. P., Vishnyakova, E. K., 2015. Major and trace elements in peat profiles in Western Siberia: impact of the landscape context, latitude and permafrost coverage. Appl. Geochem 53, 53-70. http://dx.doi.org/10.1016/j.apgeochem.2014.12.004.

Sudakov, I. A., Bobylov, L. P., Beresnev, S. A., 2011. Modeling of thermal regime of permafrost during contemporary climate change. Vestnik Sankt-Peterburgskogo universiteta, Nauki o Zemle 7(1), 81-88. (In Russian)

Trofimova, I. E., Balybina, A. S., 2014. Classification of climates and climatic regionalization of the West-Siberian plain. Geography and Natural Resources 35(2), 114-122. https://doi.org/10.1134/S1875372814020024.

Vonk, J. E., Tank, S. E., Bowden, W. B., Laurion, I., Vincent, W. F., Alekseychik, P., Amyot, M., Billet, M. F., Canario, J., Cory, R. M., Deshpande, B. N., Helbig, M., Jammet, M., Karlsson, J., Larouche, J., MacMillan, G., Rautio, M., Walter, A. K. M., Wickland, K. P., 2015. Reviews and syntheses: Effects of permafrost thaw on Arctic aquatic ecosystems. Biogeosciences 12(23), 7129-7167. https://doi.org/10.5194/bg-12-7129-2015.

Vorobyev, S. N., Pokrovsky, O. S., Kirpotin, S. N., Kolesnichenko, L. G., Shirokova, L. S., Manasypov, R. M., 2015. Flood zone biogeochemistry of the Ob River middle course. Appl. Geochem. 63, 133-145. https://doi.org/10.1016/j.apgeochem.2015.08.005.

Vorobyev, S., Pokrovsky, O., Serikova, S., Manasypov, R., Krickov, I., Shirokova, L., Lim, A., Kolesnichenko, L. G., Kirpotin, S. N., Karlsson, J., 2017. Permafrost boundary shift in western Siberia may not modify dissolved nutrient concentrations in rivers. Water 9(12), 985. https://doi.org/10.3390/w9120985.

Vorobyev, S. N., Pokrovsky, O. S., Kolesnichenko, L. G., Manasypov, R. M., Shirokova, L. S., Karlsson, J., Kirpotin, S. N. Biogeochemistry of dissolved carbon, major and trace elements during spring flood periods on the Ob River. Hydrol. Process. 33(11), 1579-1594. https://doi.org/10.1002/hyp.13424. In press.

Wrona, F. J., Johansson, M., Culp, J. M., Jenkins, A., Mård, J., Myers-Smith, I. H., Prowse, T. D., Vincent, W. F., Wookey, P. A., 2016. Transitions in Arctic ecosystems: Ecological implications of a changing hydrological regime. J. Geophys. Res.-Biogeo. 121(3), 650-674. https://doi.org/10.1002/2015JG003133.

Zhang, Y., Jacob, D. J., Dutkiewicz, S., Amos, H. M., Long, M. S., Sunderland, E. M., 2015. Biogeochemical drivers of the fate of riverine mercury discharged to the global and Arctic oceans. Global Biogeochem. Cy. 29(6), 854-864. http://dx.doi.org/10.1002/2015GB005124.

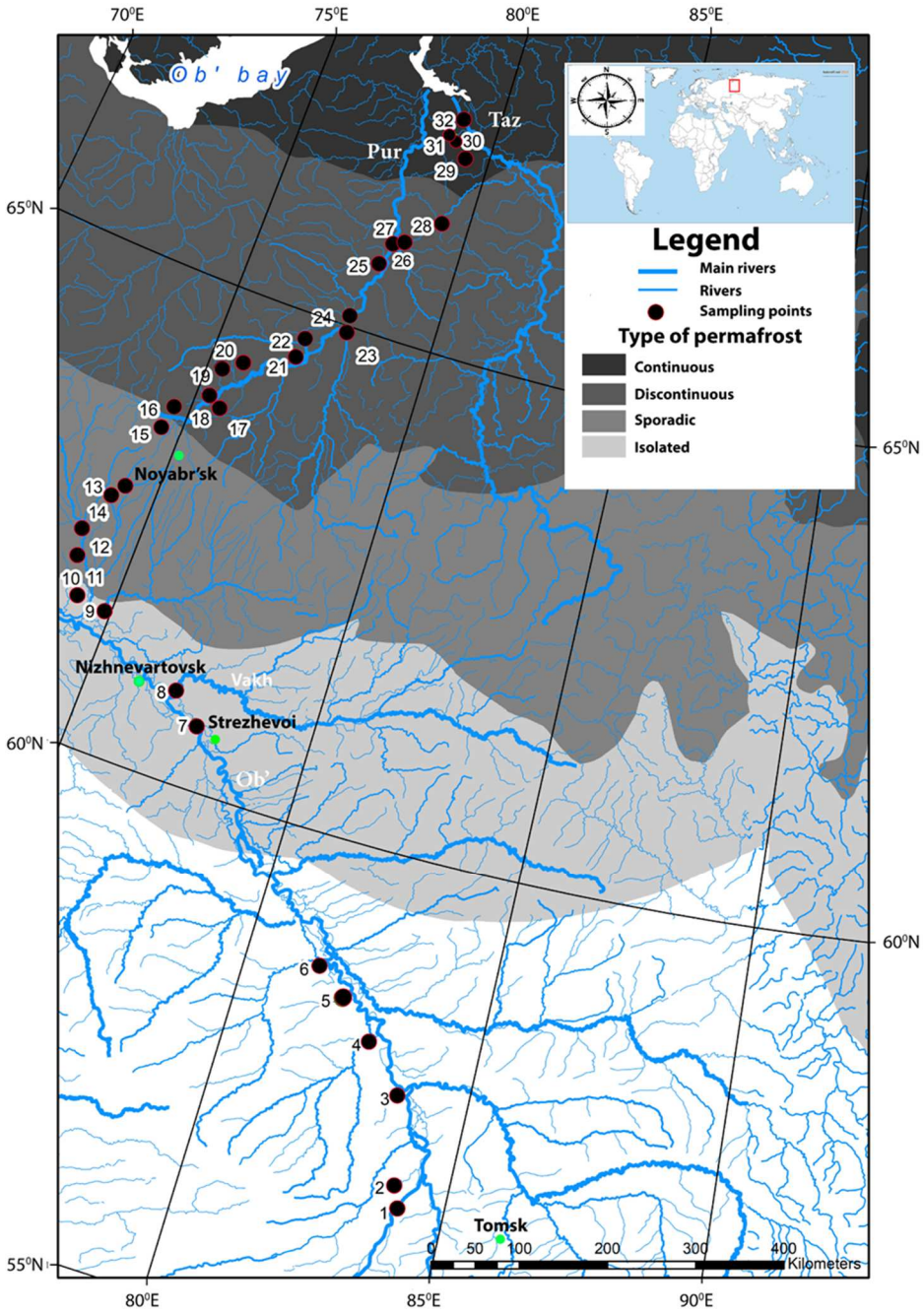

795

796 **Fig. 1.** Sampling sites and physico-geographical context of WSL territory investigated in this

797 work.

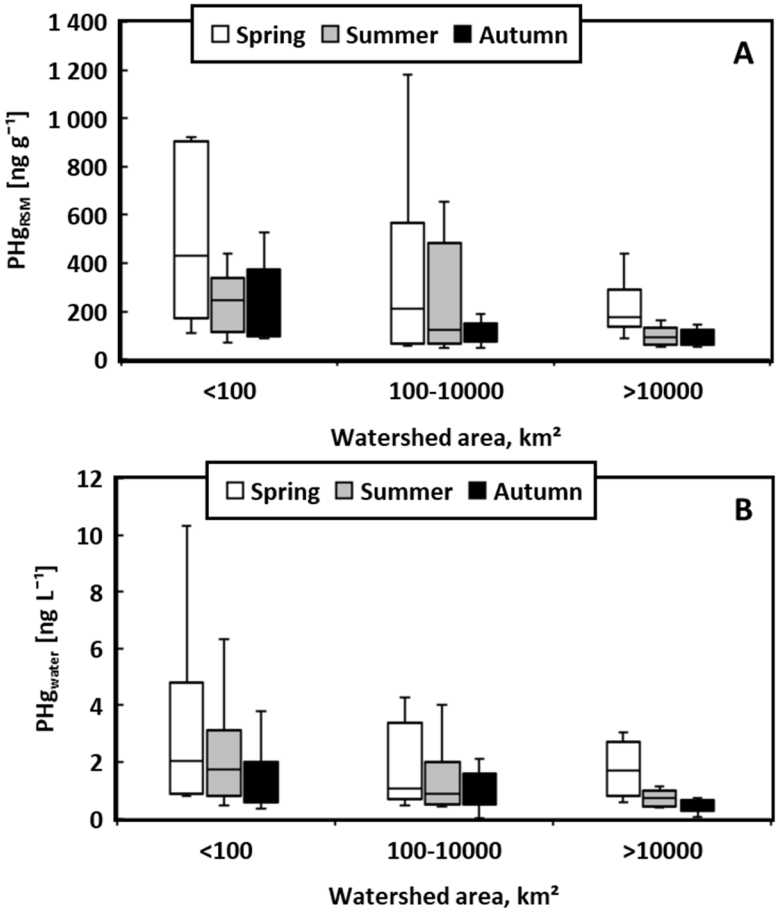

Fig. 2. Particulate (> 0.45 µm) Hg concentration (median ± IQR) in the river suspended matter (PHg_{RSM}, A) and riverwater (PHg_{water}, B) as a function of river watershed size.

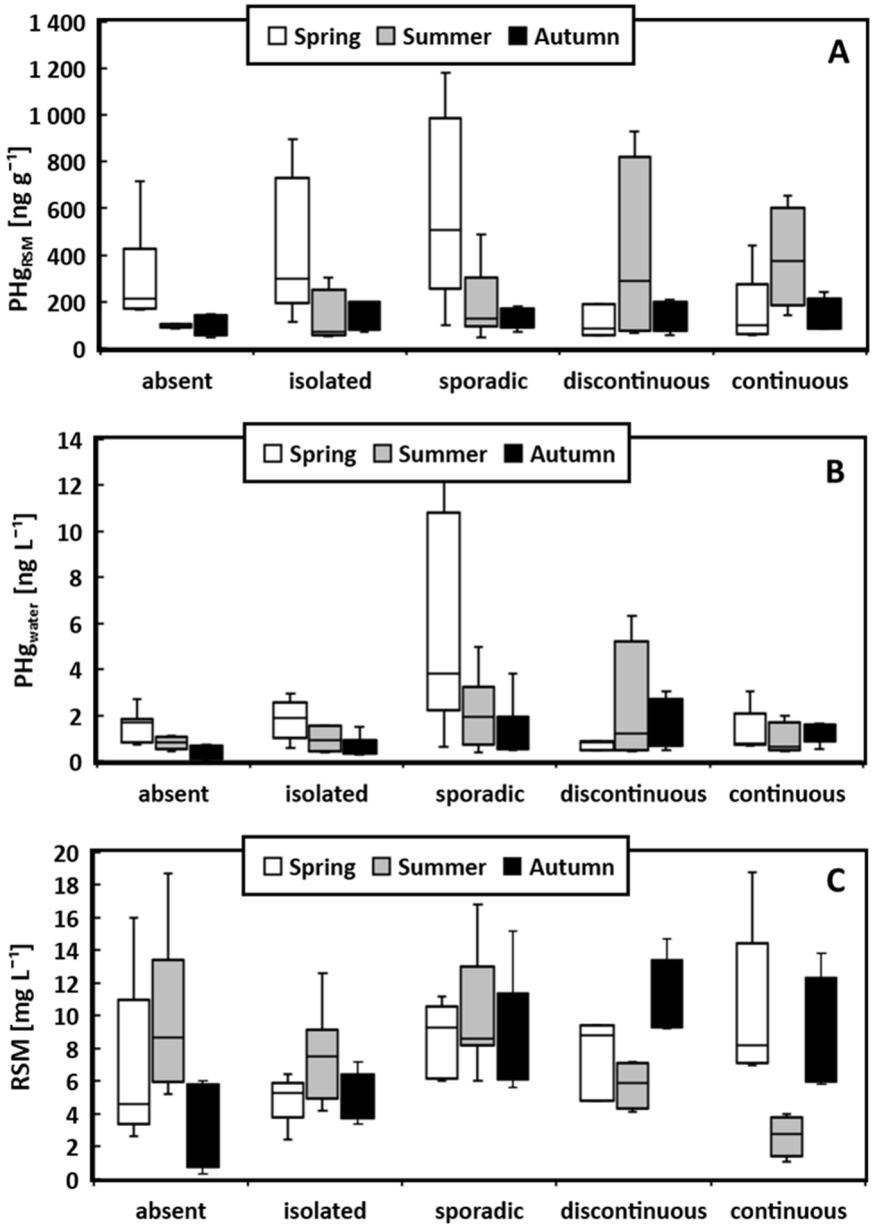

Fig. 3. Box plot of median and first and third quartiles (25 and 75%) of PHg_{RSM} (A) and PHg_{water} (B) in five permafrost zones over three seasons. A disconnect between PHg_{RSM} and PHg_{water} in discontinuous and continuous permafrost regions in summer is due to lower bulk RSM concentration in northern rivers during this period of the year (C).

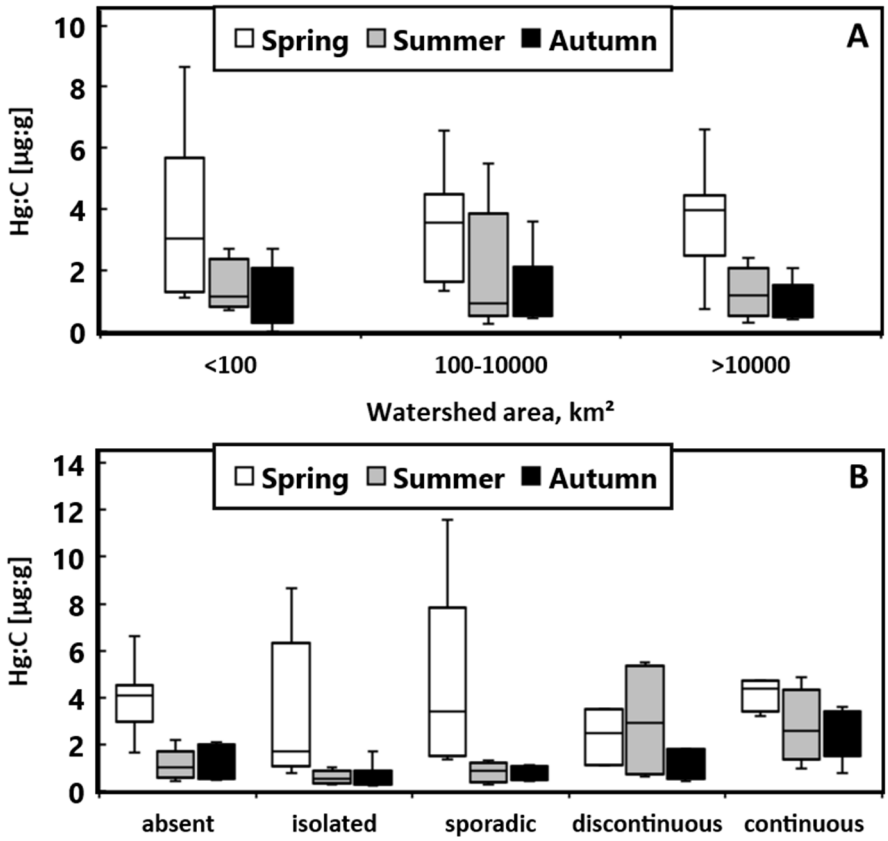

827

828

829

830 **Fig. 4.** The mass ratio Hg:C (µg g^{-1}) for rivers and streams of different size (A) and type of

831 permafrost distribution (B).

832

833

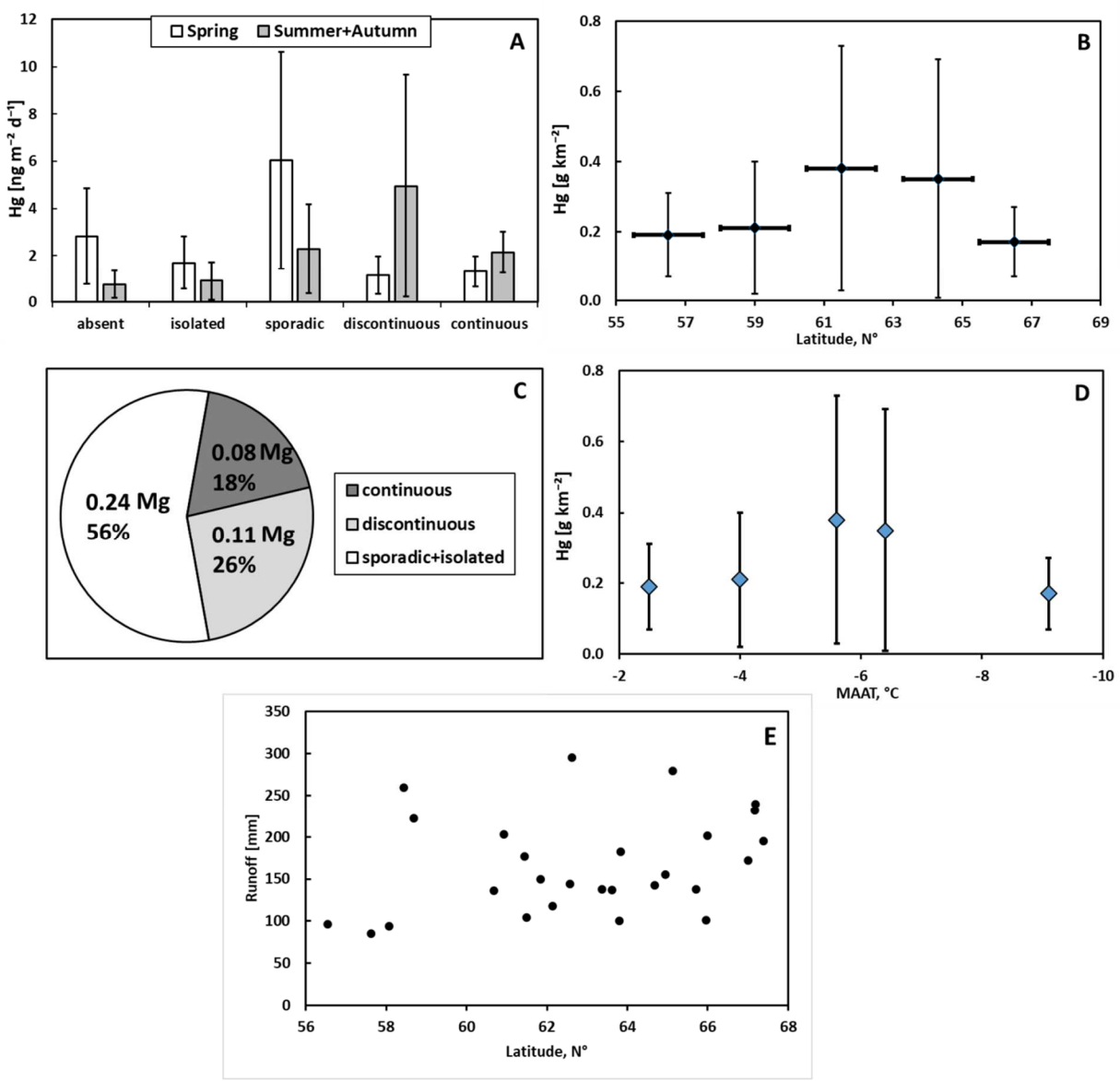

Fig. 5. Watershed surface-normalized PHg_{water} export yields during high flow (spring, May and June) and low flow (4 months, July to October) in 5 permafrost zones (**A**) the total open-water period PHg flux (6 months, May to October) across a 2-degree latitude grid (**B**). **C**, The partial contribution and PHg export in Mg of three main permafrost zones of the WSL during 6 months of open water period. **D,** Relationship between the yield of PHg by WSL rivers and the MAAT (mean annual air temperature) of the watershed (binned to 5 permafrost zones**).** The error bars in A, B and D represent ±1 S.D. Note that during open water period (May to October), the river runoff from the WSL territory is maximal in spring and independent on latitude **(E).**

Table 1. Median (± IQR) and mean (± SD) values of PHg concentration in water (PHg_{water}, ng L^{-1}) and in RSM (PHg_{RSM}, ng g^{-1}) as well as the ratio of Hg:C in RSM (µg g^{-1}) for 5 permafrost zones and 3 seasons across the WSL transect. For the permafrost-affected zone of WSL, we recommend annual mean Hg concentration equals to 1.8 (median 1.2) ng Hg L^{-1} in water and 246 (median 139) ng Hg g^{-1} in RSM. The discharge-weighed Hg:C ratio is estimated as 2.7±0.5 µg g^{-1}.

Season	Variable	Permafrost free	Permafrost			
		Absent	Isolated	Sporadic	Discontinuous	Continuous
Spring	PHg_{water}, ng L^{-1}	1.7±1.0 1.6±0.7	1.9±0.7 1.8±0.9	3.8±7.6 5.6±4.6	0.8±0.4 0.7±0.2	0.8±0.3 1.3±1.0
Spring	PHg_{RSM}, ng g^{-1}	211±257 304±204	299±290 430±308	509±617 588±400	86±134 110±70	97±42 155±161
Spring	Hg:C, µg g^{-1}	4.1±1.5 4.0±1.5	2.7±5.2 3.3±3.2	2.5±5.0 4.6±3.9	2.5±2.4 2.4±1.2	4.4±1.1 4.1±0.7
Summer	PHg_{water}, ng L^{-1}	0.8±0.4 1.0±0.8	0.7±0.8 1.0±0.6	1.7±1.4 2.0±1.6	1.2±3.7 2.3±2.8	0.7±0.8 0.9±0.7
Summer	PHg_{RSM}, ng g^{-1}	94±11 99±28	65±79 137±110	159±178 197±142	288±626 394±405	372±323 385±216
Summer	Hg:C, µg g^{-1}	1.1±1.0 1.1±0.6	0.6±0.2 0.6±0.3	0.9±0.7 1.1±1.0	2.9±4.3 3.0±2.5	2.6±2.0 2.7±1.6
Autumn	PHg_{water}, ng L^{-1}	0.3±0.5 0.5±1.3	0.6±0.4 0.7±0.4	0.8±0.9 1.4±1.1	1.4±1.4 1.6±1.1	1.4±0.3 0.2±0.4
Autumn	PHg_{RSM}, ng g^{-1}	151±118 151±157	93±33 152±144	142±124 148±89	151±91 141±65	154±101 151±67
Autumn	Hg:C, µg g^{-1}	1.3±1.3 1.3±0.7	0.5±0.2 0.6±0.5	0.5±0.4 0.9±0.7	1.3±1.0 1.2±0.6	2.4±0.9 2.4±1.1

Footnote : the median values are given in the numerator and the mean values are given in the denominator.

Particulate Hg in Siberian rivers